ULTRA SONO GRAPHY

# Ultrasonography and dual-energy computed tomography: impact for the detection of gouty deposits

Christoph Schwabl[1], Mihra Taljanovic[2], Gerlig Widmann[1], James Teh[3], Andrea S. Klauser[1]

[1]Department of Radiology, Medical University Innsbruck, Innsbruck, Austria; [2]Department of Medical Imaging, Banner University Medical Center, The University of Arizona, College of Medicine, Tucson, AZ, USA; [3]Department of Radiology, Nuffield Orthopaedic Centre, Oxford University Hospitals NHS Trust, Oxford, UK

REVIEW ARTICLE

https://doi.org/10.14366/usg.20063
pISSN: 2288-5919 • eISSN: 2288-5943
Ultrasonography 2021;40:197-206

Ultrasonography (US) and dual-energy computed tomography (DECT) are useful and sensitive diagnostic tools to identify monosodium urate deposits in joints and soft tissues. The purpose of this review is to overview the imaging findings obtained by US and DECT in patients with gout, to understand the strengths and weaknesses of each imaging modality, and to evaluate the added value of using both modalities in combination.

Keywords: Gout; Gouty arthritis; Dual energy computed tomography; Ultrasonography; CPPD; MSU deposits

Received: May 8, 2020
Revised: September 27, 2020
Accepted: October 2, 2020

Correspondence to:
Andrea S. Klauser, MD, Department of Radiology, Medical University Innsbruck, Anichstrasse 35, A-6020 Innsbruck, Austria

Tel. +43-512-504-27088
Fax. +43-512-504-27006
E-mail: andrea.klauser@i-med.ac.at

## Introduction

With a prevalence of approximately 2% among men and 1% among women in industrialized nations, gout has become a major cause of musculoskeletal pain and arthritis. Its incidence has tripled over recent decades and it is now reported to be the most common form of inflammatory arthritis globally [1,2]. Gout is a form of inflammatory arthritis characterized by the deposition of monosodium urate (MSU) crystals in joints, cartilage, and soft tissues, which can lead to formation of tophi and joint damage [3]. Peripherally located structures such as the great toe and the ears are more commonly involved than the axial skeleton [4]. Structures of the lower limbs are especially frequently affected by gout, which has a predilection for the first metatarsophalangeal (MTP) joint. This is classically described as podagra, and is reported in up to 80% of untreated patients [5]. A recent survey showed that gout presented with single joint involvement in more than 90% of patients, whereas fewer than 1% of patients presented with gout affecting more than 4 joints [6].

Apart from intra-articular deposits, gout frequently affects tendons, where MSU deposits may be intratendinous, peritendinous, or at the enthesis [7–12]. Recently, Dalbeth et al. [13] evaluated the frequency and pattern of tendon and ligament involvement in the foot of tophaceous gout patients by dual-energy computed tomography (DECT). These authors observed that tendon involvement occurred in about 10.8% of cases, with the most affected tendon being the Achilles. Interestingly, MSU crystal deposition occurred both in the tendon substance and at the enthesis more frequently than in



How to cite this article:
Schwabl C, Taljanovic M, Widmann G, Teh J, Klauser AS. Ultrasonography and dual-energy computed tomography: impact for the detection of gouty deposits. Ultrasonography. 2021 Apr;40(2):197-206.

isolation at either of these sites [13,14]. The clinical presentation of gout includes recurrent episodes of acute arthritis with a rapid onset of severe pain, swelling and erythema. Gout has a strong association with cardiovascular diseases and hyperuricemia [15].

Demonstrating MSU crystals in the joint fluid or in a tophus by puncture and polarizing microscopy is the gold standard for the diagnosis of gout [16,17]. However, this method is invasive and not always feasible, which has led to the increasing role of ultrasonography (US) and DECT in detecting gout [15,18–23]. Both US and DECT have been included in the 2015 American College of Rheumatology (ACR) classification criteria, along with radiographs, elevated serum urate levels, clinical evidence of tophus, and MSU crystals in synovial fluid analysis [24]. Bongartz et al. [19] showed that DECT has a significant impact on clinical decision-making when gout is suspected. Since a diagnosis of gouty arthritis typically results in therapeutic steps that are markedly distinct from those used to address other types of inflammatory arthritis, failure to detect MSU deposition can result in exposure to unnecessary and ineffective treatment strategies. Alternative tests for the detection of MSU crystals, which could aid clinicians in challenging diagnostic situations, would therefore be desirable. In studies by Dalbeth [15] and Zhang et al. [20], DECT was advocated as an advanced technique for longitudinal follow-up in the monitoring of tophus size regression as a marker of treatment response [25,26]. Furthermore, DECT is very useful for the detection of MSU deposits in structures that cannot be easily aspirated, such as tendons [13].

US has been suggested as the first-line imaging modality of choice for the diagnosis and management of gout [27–29]. High-frequency transducers (12–18 MHz) provide high-resolution imaging with the unique ability to depict tiny amounts of MSU deposits on the cartilage surfaces before larger deposits develop. The advantages and reliability of using both US and DECT in conjunction for the diagnosis of gout will be addressed in this review.

## Ultrasonography

On US, MSU deposits can have several different appearances.

### Double Contour Sign

The double contour (DC) sign is defined as an abnormal hyperechoic band over the superficial margin of the hypoechoic articular hyaline cartilage, independent of the angle of insonation, which may be homogeneous or inhomogeneous, irregular or regular, and continuous or intermittent. There may be posterior acoustic shadowing, depending on both the amount and density of the MSU deposits. The DC sign can be distinguished from the cartilage interface sign by adjustment of the transducer position. The cartilage interface sign is detectable only when the US beam is perpendicular to the cartilage surface. It appears as a subtle hyperechoic line, which is thinner than the underlying osteochondral interface. This sign should be interpreted with care since posterior acoustic enhancement can be generated by an effusion, which might be present in a joint affected by gout. With the DC sign, the presence of MSU deposits on the cartilage surface generates focal or diffuse hyperechoic enhancement of the superficial margin, which can be detected even when the outer cartilage margin is not insonated perpendicular to the probe (Fig. 1) [30,31]. The thickness of the DC sign should be similar to the cortex; however, in early stages it may be thinner than the cortex.

### Snowstorm Sign and Tophi

MSU crystals may also form aggregates and appear as heterogeneous hyperechoic foci. Larger, dense aggregates develop into hypoechoic to hyperechoic inhomogeneous tophi, which have a cloudy appearance, with a hypoechoic or anechoic rim [25]. De Avila Fernandes et al. [32] reported that chronic tophi are mainly hyperechoic (96.3%). Of these, 37.6% are hyperechoic and heterogeneous and 32.6% are heterogeneous with calcification (Fig. 2A, B). US is unable to differentiate between MSU crystal depositions and calcifications, which can be achieved by DECT. Depending on the density of the MSU aggregates, partial or complete posterior acoustic shadowing, similar to that seen with calcium deposits, can be observed.

The snowstorm sign is caused by hyperechoic microtophi within a joint effusion. The differential diagnosis includes debris in an

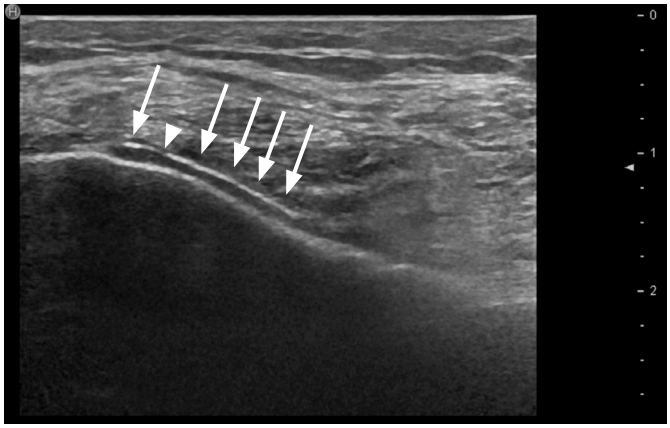


Fig. 1. **Double contour (DC) sign in an ultrasonography (US) scan of the knee.** Longitudinal US shows a DC sign (arrows) in a patient with gouty arthritis of the knee, with a hyperechoic band over the articular cartilage (hypoechoic) of the medial condyle. Note: The DC sign has the same thickness as the cortical bone, and is continuous apart from a small defect (arrowhead).

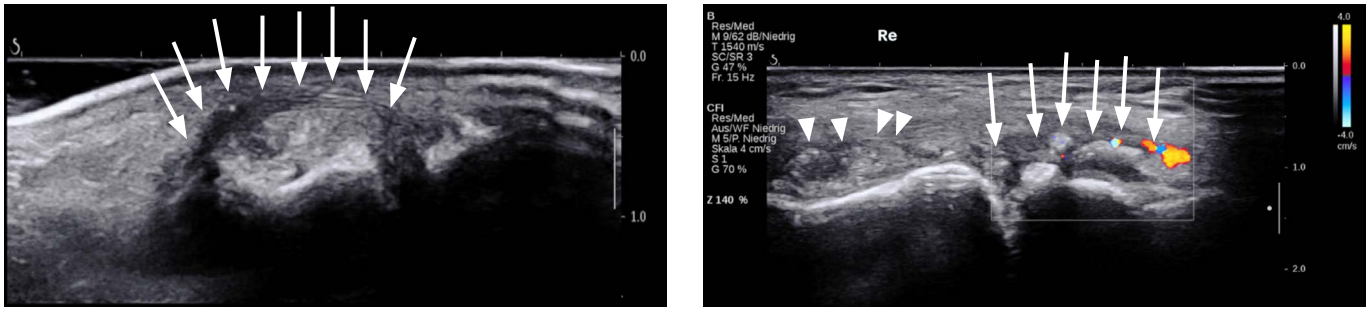


A B

Fig. 2. Typical appearance of podagra on ultrasonography (US).
A. Longitudinal US of the first metatarsophalangeal joint (MTP 1) shows a hyperechoic tophus with a surrounding hypoechoic rim (arrows), present in a patient with podagra. B. Longitudinal US of MTP 1 shows a snowstorm appearance (arrowheads) and tophus formation with a surrounding anechoic rim (arrows) with hyperemia.

osteoarthritic joint or synovial chondromatosis, which can have a similar appearance to the snowstorm sign, as described by several authors [33–36]. Aggregates and tophi are most useful when seen in conjunction with the DC sign. Standing alone, the findings may be difficult to differentiate from calcium pyrophosphate dihydrate (CPPD) crystal deposition disease. It should be noted that in patients with full-thickness cartilage loss, as seen in advanced osteoarthritis, no DC sign can be observed because of the absent hypoechoic cartilaginous layer.

### Erosions

Bony erosions can be seen on high-resolution US and appear as defects in the hyperechoic cortical bone, which are detectable in two perpendicular planes (Fig. 3A). US has been proven to be considerably more sensitive than plain radiographs for detecting erosions in rheumatoid arthritis (RA), as well as in gout [37]. Typically, gouty erosions are irregular, with overhanging margins, and are located at the joint margins, closer to the diaphysis than the erosions of RA. However, DECT gives a more comprehensive overview of intra-articular tophi, periarticular tophi, "empty" old erosions, and erosions filled with MSU deposits (Fig. 3B, C) [38]. In addition, US is also capable of detecting the inflammatory aspects of MSU deposits, including synovitis, tenosynovitis, and soft tissue inflammation, and hence can be used to monitor the efficacy of anti-inflammatory therapies [39].

## Dual-Energy Computed Tomography

Non-contrast DECT has high sensitivity and specificity for detecting MSU deposits in patients with suspected gout when compared to the gold standard of synovial fluid analysis by polarized microscopy. A recent meta-analysis of the accuracy of DECT for gout diagnosis was performed by Lee and Song [40]. In the eight studies analyzed, which included 510 patients and 268 controls, the pooled specificity and sensitivity of DECT were 93.7% and 84.7%, respectively [40,41]. DECT scanning is rapid and noninvasive, and enables multiple joints to be imaged on a single scan without the use of contrast agents [42]. Data are acquired at 80 and 140 kV with a plot of the attenuation of each voxel at 80 kV (y-axis) against attenuation at 140 kV (x-axis). The pixels containing calcium and sodium urate can be separated and presented as a color image for easy identification. Although the color coding can vary across manufacturers, the most common software color codes are green for MSU deposits, lavender for cortical bone, and pink for trabecular bone. These color-coded images are displayed as an overlay on either two-dimensional conventional gray-scale computed tomography images or as three-dimensional volume-rendered images [41] (Fig. 4). DECT can therefore provide color-coded information about the composition of certain materials, including urate, calcium pyrophosphate (CPPD), and hydroxyapatite (HADD). In addition to the visualization of MSU deposits, automated volume assessment tools that allow reliable measurements of urate deposition within a field of interest are available, which may be useful for therapeutic follow-up [43].

According to the ACR/European League Against Rheumatism guidelines, nail bed deposits, sub-millimeter deposits, skin deposits, and deposits obscured by motion, beam hardening, and vascular artifacts should not be classified as positive findings [24]. These artifacts were also described by Mallinson et al. [44], who concluded that the appearance of artifacts was especially dependent on the postprocessing protocols that were used. Park et al. [45] concluded that setting the minimum attenuation to a higher value of 150 Hounsfield units (HU) in their study reduced the frequency of artifacts, and that adding a tin filter to DECT greatly reduced their occurrence. In a study by Hu et al. [46] DECT had a specificity of

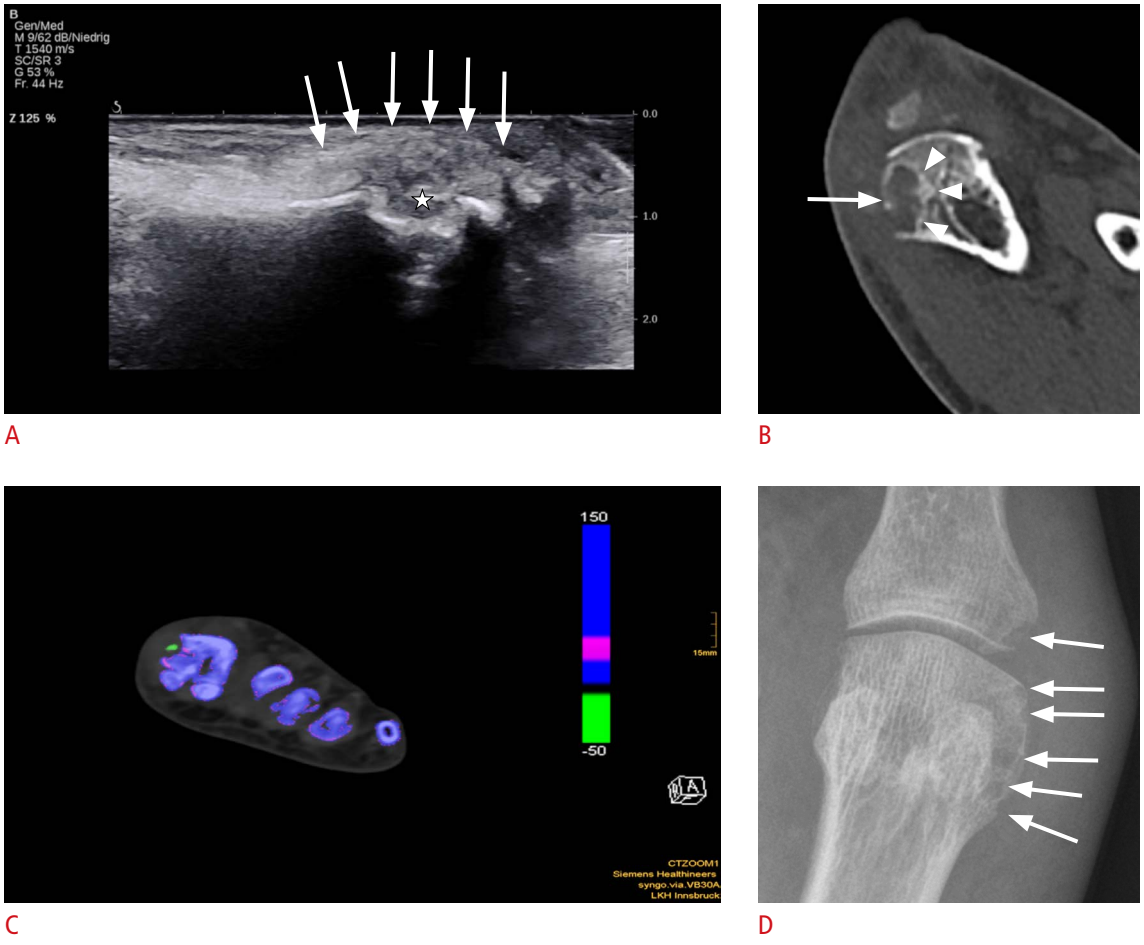


Fig. 3. Bone erosion in a patient with podagra.
A. Longitudinal ultrasonography (US) of first metatarsophalangeal joint shows bone erosion (star) of the head of the first metatarsal head in a patient with podagra. Tophus outlined by arrows. B. A corresponding computed tomography scan shows the bone erosion (arrow), as seen on US, but with better delineation of size and intraosseous extent (arrowheads). C. Axial dual-energy computed tomography shows a color-coded green monosodium urate deposit within the erosion. D. The same bone erosion is pictured in a radiographic image (arrows).

about 92.7%, resulting in a false positive rate of 7.3%. Therefore the results should be interpreted carefully [46]. Furthermore, the radiation dose is generally low, in the range of 0.1 mSv, depending on the anatomical region and the patient's body habitus. DECT may also demonstrate cardiovascular MSU deposits, which might have implications for patients who are at risk of cardiovascular disease [47].

## US and DECT in Conjunction

In 2014, Sivera et al. [48] conducted a systematic review of clinical, laboratory, and imaging findings in clinically suspected gout patients and showed that clinical features had low diagnostic utility, except for the presence of tophi on physical examination (likelihood ratio [LR], 15.6 to 30.9). US demonstrated a better performance than clinical features when using the DC sign (LR, 13.6). DECT was also found to be superior to clinical examinations (LR, 9.5) [48].

The relative value of US and DECT has been evaluated for gout in the first MTP joint, as well as the knee and the wrist, by comparing two different postprocessing protocols for DECT with US. Seventy-five consecutive patients with podagra (66 men and nine women; mean age, 65.6 years; age range, 33 to 88 years) and 75 control subjects with first MTP joint osteoarthritis (49 men and 26 women; mean age, 63.0 years; age range, 35 to 87 years) prospectively underwent US and DECT of the MTP joint between 2016 and 2018. Two Syngo.via postprocessing DECT protocols were utilized with different minimum attenuation thresholds of 150 HU (DECT 150 protocol) versus 120 HU (DECT 120 protocol). The same maximum attenuation threshold (500 HU) was used with a constant kilovoltage setting at 80 and 140 kV. The conventional postprocessing DECT 150 protocol yielded positive results for tophus

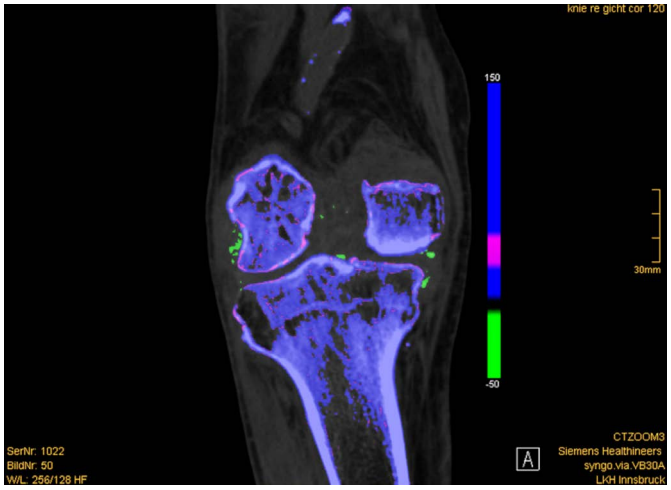


**Fig. 4. Monosodium urate (MSU) deposit in a dual-energy computed tomography (DECT) of the knee.** Coronal DECT shows color-coded green MSU deposits in the right knee affecting the medial and lateral collateral ligaments, cruciate ligaments, and intracondylar fossa.

detection in 55 of 75 patients (73.3%) with podagra, whereas the postprocessing DECT 120 protocol detected MSU deposits in all 75 patients (100%). Tophus size assessed using the DECT 120 protocol showed a closer correlation with tophus size as detected by US ($P<0.01$) [49].

In contrast to the excellent accuracy of US in detecting gouty arthritis of the first MTP joint, its accuracy in the knee and the wrist is lower, as these joints are less accessible. A study that compared DECT and US findings in patients with suspected gouty knee arthritis included 65 patients (52 men and 13 women; median age, 61.7 years; range, 38 to 87 years). DECT identified gout as the final diagnosis in 52 of 65 patients (80.0%). US detected gout in 31 of 52 patients (sensitivity, 59.6%) and produced findings negative for gout in seven of 13 patients (specificity, 53.8%). The DC sign on US was positive for gout in 23 of 52 patients (44.2%) and negative in 12 of 13 patients (92.3%).

Similar results were obtained in patients presenting with suspected gouty hand and wrist arthritis, as DECT could identify a final diagnosis of gout in 97 of 180 patients (53.9%). An alternative diagnosis was confirmed in 83 patients. US showed a sensitivity of 70.1% (extra-articular: 42.5%, $P<0.001$; intra-articular: 80.3%, $P=0.14$) and a specificity of 51%. The DC sign was present in 58 of 61 patients with a positive US study for intra-articular gout (95.1%) [23,50].

Although US and DECT have a high sensitivity in detecting gouty arthritis, there are some limitations to each modality. A major differential diagnosis of MSU deposits is CPPD, which is characterized by the accumulation of CPPD crystals in articular and periarticular tissues [51]. On US, CPPD can be detected with a high sensitivity and specificity. Chondrocalcinosis is visualized as thin intra-cartilaginous hyperechoic bands parallel to the surface of the articular cartilage [52]. Furthermore, punctate hyperechoic bands may be observed in regions of fibrocartilage, such as the triangular fibrocartilage complex or menisci. CPPD aggregates are located within the cartilage layer, whereas MSU deposits are typically localized on the outer hyaline cartilage surface [53–55] (Fig. 5). Homogeneous hyperechoic nodular or oval deposits in the joint space or bursa, representing free crystal aggregates, may also be present in CPPD and HADD [56] (Fig. 6). These echogenic deposits may be very similar to MSU deposits, making differentiation by US alone difficult if the DC sign is not present. Furthermore, in advanced gouty disease, extensive tophi causing dorsal shadowing might be present, obscuring the DC sign. Under these circumstances, either synovial fluid aspiration with microscopy or DECT are the only reliable techniques for a definitive diagnosis.

Another advantage of using DECT following first-line US is the detection of extra-articular MSU deposits (e.g., in the tendons), which cannot be differentiated from HADD by US alone. For MSU deposits in regions not accessible by US, such as the cruciate ligaments of the knee or the subtalar joint, DECT also offers an excellent overview of MSU deposits (Fig. 7).

DECT can also detect subclinical MSU deposits [43,57]. Discrepancies between the detection rates of US and DECT have been observed in several studies. Huppertz et al. [58] showed that DECT was slightly more specific for the diagnosis of gout than US (sensitivity, 84.6% [33 of 39 patients]; specificity, 85.7% [18 of 21 patients]; positive predictive value [PPV], 91.7% [33/36]; negative predictive value [NPV], 75.0% [18/24] for DECT vs. sensitivity, 100% [39/39 patients], specificity, 76.2% [16/21 patients]; PPV, 88.6% [39/44], and NPV 100% [16/16] for US). However, they concluded that DECT failed to detect small MSU deposits and was less sensitive than US on a joint-based evaluation because its lower spatial resolution missed crystal depositions on the cartilage surface (which represent the DC US sign). Therefore, the diagnosis of gout may be missed by DECT in patients with early disease limited to a few joints.

Small MSU deposits and those with low concentrations seem to generate false negative results on DECT. DECT detects dense tophi (corresponding to approximately 15%–20% by volume urate concentrations in the tophus) and misses less dense tophi below the detection threshold of 150 HU even if they have a considerable size. This might result in diagnostic performance discrepancies between the two modalities [59,60]. In summary therefore, using both modalities in conjunction, especially with US as the first-line examination whenever necessary, generates the best possibility of

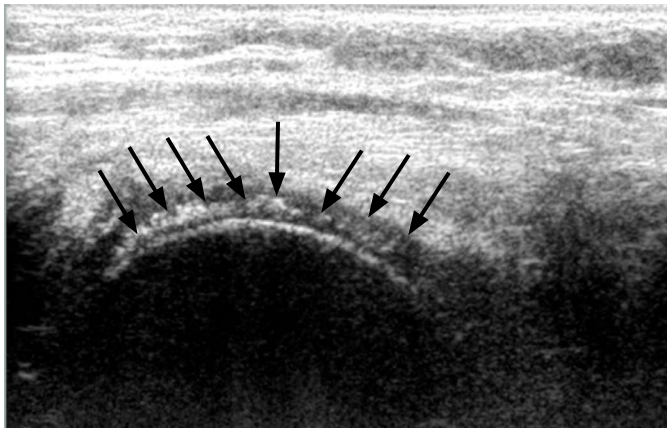

A

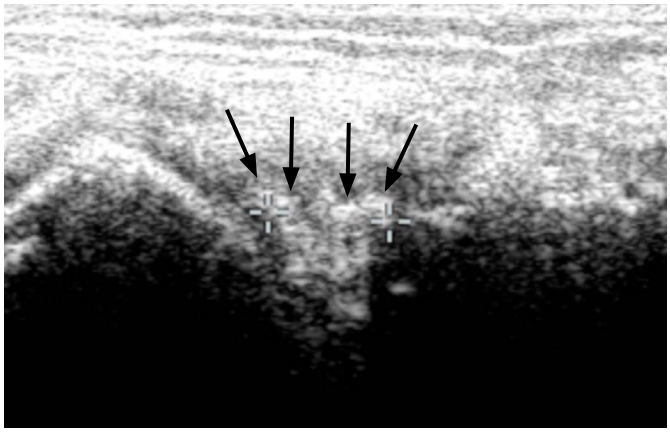

B

C

Fig. 5. A patient with calcium pyrophosphate dihydrate (CPPD) of the knee.
A. Axial ultrasonography (US) of the femoral condyle shows a thick linear deposit (arrows) within the cartilage layer, indicates high-grade CPPD. B. Parasagittal US of the lateral knee shows echogenic deposits (arrows) within the lateral meniscus. C. Corresponding X-ray of the same patient shows typical calcification (arrows) within the menisci and around the condyle.

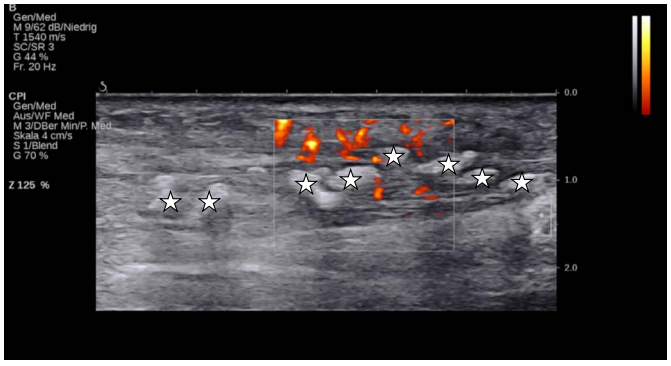

A

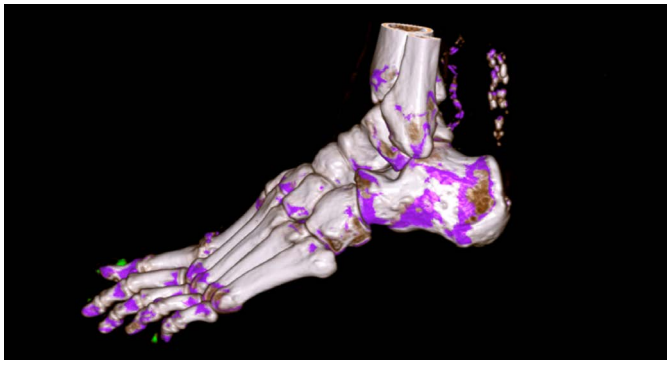

B

Fig. 6. A patient with hydroxyapatite (HADD) of the Achilles tendon.
A. Longitudinal power Doppler ultrasonography shows extensive hyperechoic aggregates (stars) in the Achilles tendon with posterior acoustic shadowing. This could also be interpreted as multiple tophi due to edema limiting the detection of the fibrillar echotexture of the Achilles tendon. B. A 3D rendered dual-energy computed tomography of the same patient confirms HADD (color-coded purple) in the Achilles tendon, without evidence of monosodium urate deposits (color-coded green). Note: Green artifacts of nails.

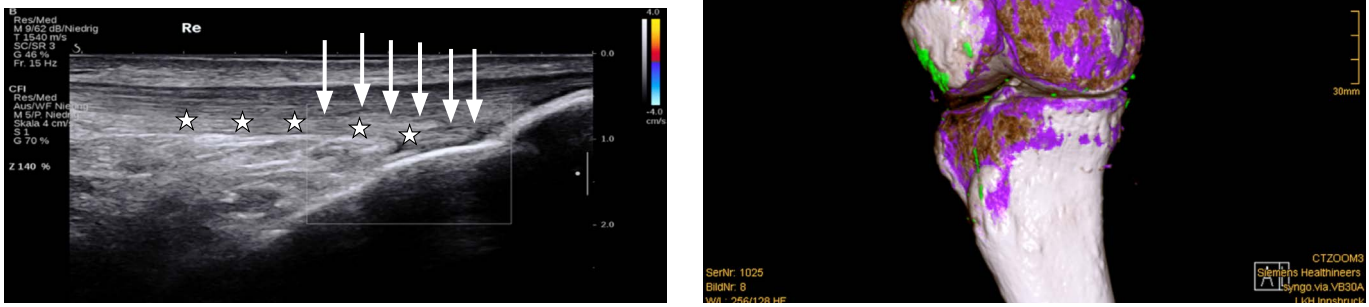

A B

Fig. 7. Extra-articular monosodium urate (MSU) deposits in the quadriceps tendon.
A. Longitudinal ultrasonography of the distal quadriceps tendon is shown. No hypervascularity or tendinosis is seen, but there are diffuse discrete hyperechoic deposits at the posterior layer of the tendon (stars). There is no dorsal shadowing, but a discrete hypoechoic halo is present (arrows). The extent of the abnormality only became apparent retrospectively after performing dual-energy computed tomography (DECT). B. Sagittal three-dimensional rendered DECT demonstrates color-coded green MSU deposits along the quadriceps tendon and the prepatellar region. Furthermore, discrete MSU deposits (green) are visible in the infrapatellar tendon, medial collateral ligaments, and menisci.

not missing any positive findings.

For this reason, we provided a standardized algorithm, where US is the first-line investigation for patients with a high pre-test probability of gout due to distinct clinical features, followed by DECT if the US findings are inconclusive. This approach can obviate the need for radiography and synovial fluid puncture and aligns with the recommendations of other authors (Table 1) [61–63].

## Conclusion

US and DECT are noninvasive imaging modalities with excellent sensitivity and specificity for detecting MSU deposits. In some patients, it may be necessary to use them both in conjunction to improve the diagnostic imaging algorithm for gout. US is cheaper and more widely available than DECT, and has been shown to be more sensitive for early disease and when low concentrations of MSU deposits are present. It also allows the detection of soft tissue inflammation, which may be useful for assessing the response to therapy. DECT may not be available at the same day for most institutions, and clinicians may want to initiate therapy. It is therefore proposed to use US as a first line of investigation in patients with suspected acute gout. However, DECT has the advantage of greater sensitivity and specificity than US in the detection of MSU deposits in certain regions. With a standardized algorithm using DECT after US in unclear cases, high accuracy can be achieved in the diagnosis or exclusion of gout, obviating the need for invasive procedures.

Table 1. Proposed diagnostic algorithm

| First-line US | US finding | Implication |
|---|---|---|
| US positive | DC sign<br>Tophus<br>Aggregates+DC sign | Can diagnose gout |
| US negative | No arthritis signs<br>No synovitis<br>No edema<br>No echogenic deposits or DC sign | Can exclude gout |
| US inconclusive | Arthritis of unknown origin, but high clinical suspicion of gout<br>Echogenic deposits not typically seen for gout | DECT |

US, ultrasonography; DC, double contour; DECT, dual-energy computed tomography.

ORCID: Christoph Schwabl: https://orcid.org/0000-0002-4438-9025; Mihra Taljanovic: https://orcid.org/0000-0003-1910-6545; Gerlig Widmann: https://orcid.org/0000-0002-7255-0672; James Teh: https://orcid.org/0000-0002-6111-4269; Andrea S. Klauser: https://orcid.org/0000-0002-1059-9278

### Author Contributions

Conceptualization: Schwabl C, Klauser AS, Widmann G. Data acquisition: Schwabl C, Klauser AS. Data analysis or interpretation: Schwabl C, Klauser AS, Taljanovic M, Teh J. Drafting of the manuscript: Schwabl C, Klauser AS, Teh J, Taljanovic M. Critical

revision of the manuscript: Schwabl C, Klauser AS, Widmann G, Taljanovic M, Teh J. Approval of the final version of the manuscript: all authors.

### Conflict of Interest

No potential conflict of interest relevant to this article was reported.

## References


1. Smith EU, Diaz-Torne C, Perez-Ruiz F, March LM. Epidemiology of gout: an update. Best Pract Res Clin Rheumatol 2010;24:811-827.
2. Kuo CF, Grainge MJ, Zhang W, Doherty M. Global epidemiology of gout: prevalence, incidence and risk factors. Nat Rev Rheumatol 2015;11:649-662.
3. Girish G, Melville DM, Kaeley GS, Brandon CJ, Goyal JR, Jacobson JA, et al. Imaging appearances in gout. Arthritis 2013;2013:673401.
4. Chabra I, Singh R. Gouty tophi on the ear: a review. Cutis 2013;92:190-192.
5. Perez-Ruiz F, Castillo E, Chinchilla SP, Herrero-Beites AM. Clinical manifestations and diagnosis of gout. Rheum Dis Clin North Am 2014;40:193-206.
6. Liote F, Lancrenon S, Lanz S, Guggenbuhl P, Lambert C, Saraux A, et al. GOSPEL: prospective survey of gout in France. Part I: design and patient characteristics (n = 1003). Joint Bone Spine 2012;79:464-470.
7. Peiteado D, De Miguel E, Villalba A, Ordonez MC, Castillo C, Martin-Mola E. Value of a short four-joint ultrasound test for gout diagnosis: a pilot study. Clin Exp Rheumatol 2012;30:830-837.
8. Gerster JC, Landry M, Rappoport G, Rivier G, Duvoisin B, Schnyder P. Enthesopathy and tendinopathy in gout: computed tomographic assessment. Ann Rheum Dis 1996;55:921-923.
9. Weniger FG, Davison SP, Risin M, Salyapongse AN, Manders EK. Gouty flexor tenosynovitis of the digits: report of three cases. J Hand Surg Am 2003;28:669-672.
10. Primm DD Jr, Allen JR. Gouty involvement of a flexor tendon in the hand. J Hand Surg Am 1983;8:863-865.
11. de Avila Fernandes E, Sandim GB, Mitraud SA, Kubota ES, Ferrari AJ, Fernandes AR. Sonographic description and classification of tendinous involvement in relation to tophi in chronic tophaceous gout. Insights Imaging 2010;1:143-148.
12. Yuan Y, Liu C, Xiang X, Yuan TL, Qiu L, Liu Y, et al. Ultrasound scans and dual energy CT identify tendons as preferred anatomical location of MSU crystal depositions in gouty joints. Rheumatol Int 2018;38:801-811.
13. Dalbeth N, Kalluru R, Aati O, Horne A, Doyle AJ, McQueen FM. Tendon involvement in the feet of patients with gout: a dual-energy CT study. Ann Rheum Dis 2013;72:1545-1548.
14. Ventura-Rios L, Sanchez-Bringas G, Pineda C, Hernandez-Diaz C, Reginato A, Alva M, et al. Tendon involvement in patients with gout: an ultrasound study of prevalence. Clin Rheumatol 2016;35:2039-2044.
15. Dalbeth N. Management of gout in primary care: challenges and potential solutions. Rheumatology (Oxford) 2013;52:1549-1550.
16. McQueen FM, Chhana A, Dalbeth N. Mechanisms of joint damage in gout: evidence from cellular and imaging studies. Nat Rev Rheumatol 2012;8:173-181.
17. Buckley TJ. Radiologic features of gout. Am Fam Physician 1996;54:1232-1238.
18. Glazebrook KN, Guimaraes LS, Murthy NS, Black DF, Bongartz T, Manek NJ, et al. Identification of intraarticular and periarticular uric acid crystals with dual-energy CT: initial evaluation. Radiology 2011;261:516-524.
19. Bongartz T, Glazebrook KN, Kavros SJ, Murthy NS, Merry SP, Franz WB 3rd, et al. Dual-energy CT for the diagnosis of gout: an accuracy and diagnostic yield study. Ann Rheum Dis 2015;74:1072-1077.
20. Zhang Z, Zhang X, Sun Y, Chen H, Kong X, Zhou J, et al. New urate depositions on dual-energy computed tomography in gouty arthritis during urate-lowering therapy. Rheumatol Int 2017;37:1365-1372.
21. Finkenstaedt T, Manoliou A, Toniolo M, Higashigaito K, Andreisek G, Guggenberger R, et al. Gouty arthritis: the diagnostic and therapeutic impact of dual-energy CT. Eur Radiol 2016;26:3989-3999.
22. Klauser AS, Gruber J. Response to: "Monosodium urate crystal deposition associated with the progress of radiographic grade at the sacroiliac joint in axial SpA: a dual-energy CT study". Arthritis Res Ther 2018;20:28.
23. Klauser AS, Halpern EJ, Strobl S, Abd Ellah MM, Gruber J, Bellmann-Weiler R, et al. Gout of hand and wrist: the value of US as compared with DECT. Eur Radiol 2018;28:4174-4181.
24. Neogi T, Jansen TL, Dalbeth N, Fransen J, Schumacher HR, Berendsen D, et al. 2015 Gout classification criteria: an American College of Rheumatology/European League Against Rheumatism collaborative initiative. Ann Rheum Dis 2015;74:1789-1798.
25. Wu H, Xue J, Ye L, Zhou Q, Shi D, Xu R. The application of dual-energy computed tomography in the diagnosis of acute gouty arthritis. Clin Rheumatol 2014;33:975-979.
26. Modjinou DV, Krasnokutsky S, Gyftopoulos S, Pike VC, Karis E, Keenan RT, et al. Comparison of dual-energy CT, ultrasound and surface measurement for assessing tophus dissolution during rapid urate debulking. Clin Rheumatol 2017;36:2101-2107.
27. Swan A, Amer H, Dieppe P. The value of synovial fluid assays in the diagnosis of joint disease: a literature survey. Ann Rheum Dis 2002;61:493-498.
28. Manger B, Lell M, Wacker J, Schett G, Rech J. Detection of periarticular urate deposits with dual energy CT in patients with

acute gouty arthritis. Ann Rheum Dis 2012;71:470-472.
29. Chowalloor PV, Keen HI. A systematic review of ultrasonography in gout and asymptomatic hyperuricaemia. Ann Rheum Dis 2013;72:638-645.
30. Filippucci E, Di Geso L, Grassi W. Tips and tricks to recognize microcrystalline arthritis. Rheumatology (Oxford) 2012;51 Suppl 7:vii18-vii21.
31. Han TS, Kwack KS, Park S, Min BH, Yoon SH, Lee HY, et al. A superficial hyperechoic band in human articular cartilage on ultrasonography with histological correlation: preliminary observations. Ultrasonography 2015;34:115-124.
32. de Avila Fernandes E, Kubota ES, Sandim GB, Mitraud SA, Ferrari AJ, Fernandes AR. Ultrasound features of tophi in chronic tophaceous gout. Skeletal Radiol 2011;40:309-315.
33. Bruyn GA, Iagnocco A, Naredo E, Balint PV, Gutierrez M, Hammer HB, et al. OMERACT definitions for ultrasonographic pathologies and elementary lesions of rheumatic disorders 15 years On. J Rheumatol 2019;46:1388-1393.
34. Iagnocco A. Imaging the joint in osteoarthritis: a place for ultrasound? Best Pract Res Clin Rheumatol 2010;24:27-38.
35. Farina A, Filippucci E, Grassi W. Sonographic findings for synovial fluid. Reumatismo 2002;54:261-265.
36. Zell M, Zhang D, FitzGerald J. Diagnostic advances in synovial fluid analysis and radiographic identification for crystalline arthritis. Curr Opin Rheumatol 2019;31:134-143.
37. McQueen FM, Reeves Q, Dalbeth N. New insights into an old disease: advanced imaging in the diagnosis and management of gout. Postgrad Med J 2013;89:87-93.
38. Dalbeth N, Aati O, Kalluru R, Gamble GD, Horne A, Doyle AJ, et al. Relationship between structural joint damage and urate deposition in gout: a plain radiography and dual-energy CT study. Ann Rheum Dis 2015;74:1030-1036.
39. Rymal E, Rizzolo D. Gout: a comprehensive review. JAAPA 2014;27:26-31.
40. Lee YH, Song GG. Diagnostic accuracy of ultrasound in patients with gout: a meta-analysis. Semin Arthritis Rheum 2018;47:703-709.
41. Garner HW, Wessell DE. Gout: update on dual-energy computed tomography with emphasis on artifact identification. Curr Rheumatol Rep 2018;20:86.
42. Wang P, Smith SE, Garg R, Lu F, Wohlfahrt A, Campos A, et al. Identification of monosodium urate crystal deposits in patients with asymptomatic hyperuricemia using dual-energy CT. RMD Open 2018;4:e000593.
43. Choi HK, Al-Arfaj AM, Eftekhari A, Munk PL, Shojania K, Reid G, et al. Dual energy computed tomography in tophaceous gout. Ann Rheum Dis 2009;68:1609-1612.
44. Mallinson PI, Coupal T, Reisinger C, Chou H, Munk PL, Nicolaou S, et al. Artifacts in dual-energy CT gout protocol: a review of 50 suspected cases with an artifact identification guide. AJR Am J Roentgenol 2014;203:W103-W109.
45. Park EH, Yoo WH, Song YS, Byon JH, Pak J, Choi Y. Not all green is tophi: the importance of optimizing minimum attenuation and using a tin filter to minimize clumpy artifacts on foot and ankle dual-energy CT. AJR Am J Roentgenol 2020;214:1335-1342.
46. Hu HJ, Liao MY, Xu LY. Clinical utility of dual-energy CT for gout diagnosis. Clin Imaging 2015;39:880-885.
47. Klauser AS, Halpern EJ, Strobl S, Gruber J, Feuchtner G, Bellmann-Weiler R, et al. Dual-energy computed tomography detection of cardiovascular monosodium urate deposits in patients with gout. JAMA Cardiol 2019;4:1019-1028.
48. Sivera F, Andres M, Falzon L, van der Heijde DM, Carmona L. Diagnostic value of clinical, laboratory, and imaging findings in patients with a clinical suspicion of gout: a systematic literature review. J Rheumatol Suppl 2014;92:3-8.
49. Strobl S, Kremser C, Taljanovic M, Gruber J, Stofferin H, Bellmann-Weiler R, et al. Impact of dual-energy CT postprocessing protocol for the detection of gouty arthritis and quantification of tophi in patients presenting with Podagra: comparison with ultrasound. AJR Am J Roentgenol 2019;213:1315-1323.
50. Strobl S, Halpern EJ, Ellah MA, Kremser C, Gruber J, Bellmann-Weiler R, et al. Acute gouty knee arthritis: ultrasound findings compared with dual-energy CT findings. AJR Am J Roentgenol 2018;210:1323-1329.
51. Magarelli N, Amelia R, Melillo N, Nasuto M, Cantatore F, Guglielmi G. Imaging of chondrocalcinosis: calcium pyrophosphate dihydrate (CPPD) crystal deposition disease: imaging of common sites of involvement. Clin Exp Rheumatol 2012;30:118-125.
52. Vele P, Simon SP, Damian L, Felea I, Muntean L, Filipescu I, et al. Clinical and ultrasound findings in patients with calcium pyrophosphate dihydrate deposition disease. Med Ultrason 2018;20:159-163.
53. Filippucci E, Riveros MG, Georgescu D, Salaffi F, Grassi W. Hyaline cartilage involvement in patients with gout and calcium pyrophosphate deposition disease: an ultrasound study. Osteoarthritis Cartilage 2009;17:178-181.
54. Thiele RG, Schlesinger N. Diagnosis of gout by ultrasound. Rheumatology (Oxford) 2007;46:1116-1121.
55. Wright SA, Filippucci E, McVeigh C, Grey A, McCarron M, Grassi W, et al. High-resolution ultrasonography of the first metatarsal phalangeal joint in gout: a controlled study. Ann Rheum Dis 2007;66:859-864.
56. Miksanek J, Rosenthal AK. Imaging of calcium pyrophosphate deposition disease. Curr Rheumatol Rep 2015;17:20.
57. Dalbeth N, House ME, Aati O, Tan P, Franklin C, Horne A, et al. Urate crystal deposition in asymptomatic hyperuricaemia and symptomatic gout: a dual energy CT study. Ann Rheum Dis 2015;74:908-911.

58. Huppertz A, Hermann KG, Diekhoff T, Wagner M, Hamm B, Schmidt WA. Systemic staging for urate crystal deposits with dual-energy CT and ultrasound in patients with suspected gout. Rheumatol Int 2014;34:763-771.
59. Teh J, McQueen F, Eshed I, Plagou A, Klauser A. Advanced imaging in the diagnosis of gout and other crystal arthropathies. Semin Musculoskelet Radiol 2018;22:225-236.
60. Pascart T, Grandjean A, Norberciak L, Ducoulombier V, Motte M, Luraschi H, et al. Ultrasonography and dual-energy computed tomography provide different quantification of urate burden in gout: results from a cross-sectional study. Arthritis Res Ther 2017;19:171.
61. Girish G, Glazebrook KN, Jacobson JA. Advanced imaging in gout. AJR Am J Roentgenol 2013;201:515-525.
62. Newberry SJ, FitzGerald JD, Motala A, Booth M, Maglione MA, Han D, et al. Diagnosis of gout: a systematic review in support of an American College of Physicians Clinical Practice Guideline. Ann Intern Med 2017;166:27-36.
63. Ogdie A, Taylor WJ, Weatherall M, Fransen J, Jansen TL, Neogi T, et al. Imaging modalities for the classification of gout: systematic literature review and meta-analysis. Ann Rheum Dis 2015;74:1868-1874.